

Towards Physics-Informed PHM for Multi-component degradation (MCD) in complex systems

Atuahene Barimah¹, Octavian Niculita², Don McGlinchey³, Andrew Cowell⁴ and Billy Milligan⁵

^{1,2,3,4} *Glasgow Caledonian University, Glasgow, G4 0BA, UK*

abarim300@gcu.ac.uk, octavian.niculita@gcu.ac.uk, d.mcglinchey@gcu.ac.uk, A.Cowell@gcu.ac.uk

⁵*Howden/Chart Industries, Glasgow, Renfrew, PA4 8XJ, UK*

billy.milligan@howden.com

ABSTRACT

This study seeks to address the challenge of limited degradation data in developing Fault Detection and Isolation (FDI) models for multi-component degradation (MCD) scenarios. Utilizing a small fraction (0.05%) of a previously utilized water distribution testbed dataset in a previous publication, a weighted ensemble hybrid approach is proposed and evaluated against more established modelling approaches used in the previous publication. The proposed approach combines heuristic approximation and Physics-Informed Neural Network (PINN) methods with a recurrent neural network (RNN) model to enhance diagnostic performance for predicting MCD scenarios. The hybrid model generally outperformed other algorithms when tested on an MCD dataset, demonstrating improved diagnostic accuracy in such scenarios. Future research aims to optimize ensemble weights based on model uncertainty, further enhancing diagnostic capabilities.

1. INTRODUCTION

Data has become the story of engineering design in recent times as the availability of system data provides insights into the dynamics of any complex system. This is particularly true for developing analytics in digital twin (DT) design for asset health management applications (Lu, Xie, Parlikad, & Schooling, 2020). Figure 1 shows the nexus between the analytics developed for PHM applications and a virtual representation of a physical asset highlighting how DTs can enable PHM applications. In exploring cost mitigation strategies, different maintenance data-driven models often rely on large amounts of data to train effectively (Maass, Parsons, Puroo, Storey, & Woo, 2018). The more data is

available, the better the model can learn patterns and relationships within the data, leading to more accurate predictions or insights (Barimah, Niculita, McGlinchey, & Cowell, 2023). This helps data-driven models generalise better to unseen data the more data is available (Duriez, Brunton, & Noack, 2017). This is particularly useful when it comes to asset health management where the availability of trainable degradation data is critical in the design and execution of Prognostics and Health Management (PHM) strategies for complex systems undergoing multi-component degradation scenarios.

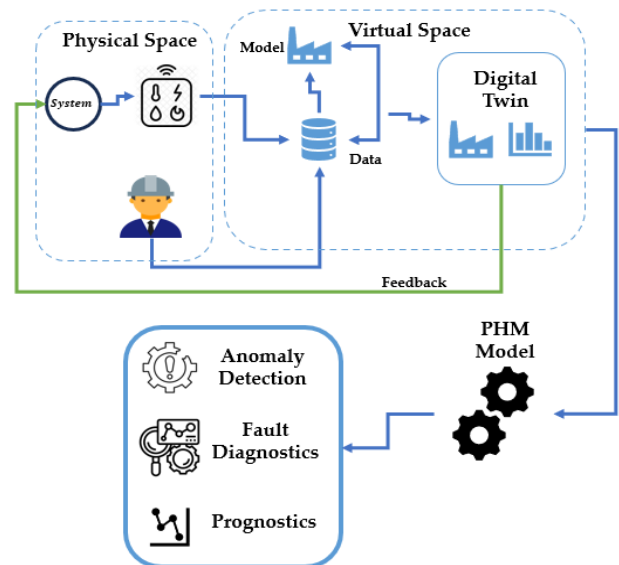


Figure 1. Relationship between DT and PHM applications.

However, obtaining asset degradation data can be expensive, time consuming, and often requires specialized equipment, sensors, or monitoring systems (Hu, Miao, Si, Pan, & Zio, 2022). Operators often rely on post-failure degradation data (Barimah, Niculita, McGlinchey, & Alkali, 2021) which enables the development of statistical-based techniques for

Atuahene Barimah et al. This is an open-access article distributed under the terms of the Creative Commons Attribution 3.0 United States License, which permits unrestricted use, distribution, and reproduction in any medium, provided the original author and source are credited.

system-level anomaly detection. The statistical-based technique alone prevents an operator from isolating the sub-systems contributing to the anomaly in the larger system. The scenario becomes even more complex when two components of the same system degrade simultaneously (very often, at different rates). Simulated degradation data calibrated with the actual physical system (Higdon, Kennedy, Cavendish, Cafeo, & Ryne, 2004) can also be used to train predictive models. However, this approach becomes limited when MCD scenarios are being considered as degradation data from the different combinations of sub-systems undergoing degradation need to be simulated to generate the required data. For complex systems with a lot of sub-systems with different operating conditions, this approach becomes untenable.

To address the issue of limited data, several authors have suggested combining the insights given by data-driven models with some physical equations that govern the dynamics of a system. Physics-Informed Neural Networks (PINNs) integrate the physics of an asset into their training process, enforcing physical constraints alongside data-driven learning. PINNs can generalize well with limited data (Cai, Mao, Wang, Yin, & Karniadakis, 2021) and have applications in various fields (Huang & Wang, 2022), making them valuable for tackling complex, multi-physics problems (Bararnia & Esmailpour, 2022) by reducing computational costs and providing insights (Rizi & Abbas, 2023). The aim and objectives of this paper are presented in section 2 below.

2. OBJECTIVES OF STUDY

This paper aims to develop and benchmark an ensemble hybrid fault detection and isolation model for components (sub-systems) undergoing multi-component degradation (MCD) scenarios in a water distribution system.

- Identify a physical equation that represents the degradation severity level of either blockages or leakages in the system.
- Design a Fault Detection and Isolation (FDI) algorithm using a PINN-enabled Hybrid model for each component in the water distribution system.
- Train all FDI models on limited degradation data and test models on test multi-component degradation scenario data from the same system at different operating conditions.
- Identify areas of model improvement and potential research.

The paper is structured as follows: Section 3 covers the methodology. Sections 4 and 5 present and discuss the results of FDI model performance. Finally, the paper concludes with contributions and future research work.

3. METHODOLOGY

3.1. System Description

Data from the dynamic behaviour of a water distribution system undergoing multi-component degradation presented in Barimah et. al (2023) was used in this report. Figure 2 below shows the water distribution experimental testbed, where an external gear pump pumps water from a main supply tank. A variable speed drive (VSD) controls the rotational speed of the pump and the motor. The system also has five (5) direct proportional valves (DPV1 to DPV5) and a solenoid shut-off valve (SHV) that were included to support the emulation of deterioration phenomena affecting five different components in a controlled manner. Data is collected from five pressure transmitters (P1, P2, P3, P4, and P5), turbine flow meters (f1 and f2), and a laser sensor to gauge the pump's speed. Table 1 lists the control valves in the system's default operating states, their respective fault codes, and the fault emulation mechanism for each component on the testbed.

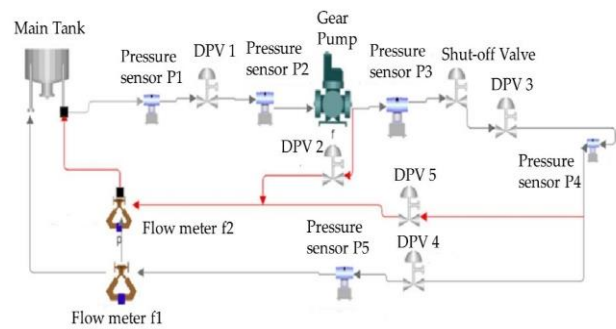


Figure 2. Water Distribution System Testbed Schematic (Barimah et. al 2023).

Table 1. Healthy condition operating state of the system's control valves and associated fault codes

Component/Fault Codes	Testbed Valves	Healthy State	Fault Emulation Mechanism
Filter/FC1	DPV 1	FO	DPV1 GC
Pump/FC2	DPV 2	FC	DPV2 GO
Valve/FC3	DPV 3	FO	DPV3 GC
Nozzle/FC4	DPV 4	FO	DPV4 GC
Pipe/FC5	DPV 5	FC	DPV5 GO

FO - Fully Open | FC - Fully Closed

GC - Gradually closing | GO - Gradually opening.

3.2. Process Data Capture

The degradation data used in the previous publication by Barimah et. al (2023) was recorded within four (4) weeks for healthy condition (HC), Single Component Degradation (SCD) and Multi-Component Degradation (MCD) scenarios between pump speeds of 700rpm and 950rpm in intervals of 50rpm. The SCD process data represents the degradation of individual components (See Table 2) with pressure and flow

measurements at $P_1, P_2 \dots P_5$ and f_1, f_2 respectively. Data logging for each faulty condition scenario last between three (3) to four (4) minutes and also starts at least 10 minutes after the process reaches steady state conditions or when there is a step change in pump speed or a change in the failure condition scenario with each data file having different sample sizes. The degradation level of severity ($0 \leq S \leq 1$) for each component on the testbed is determined by gradually closing or opening the respective direct proportional valve.

Table 2. Data capturing process with a sampling rate of 0.2s

Test period	4 consecutive weeks
Faulty Condition Scenarios (Total No of Tests)	FC0 – Healthy Condition (24) FC1–Clogged Filter (24) FC2–Degraded Pump (24) FC3–Blocked Valve (24) FC4–Blocked Nozzle (24) FC5–Leaking Pipe (24)
Pump Speed (rpm)	700/750/800/850/900/950

3.3. FDI Model Development

Sections 3.3.1 to 3.3.5 presents the process for developing physics informed fault detection and isolation (FDI) algorithms. Using limited training data, the paper also benchmarks the statistical process control (SPC), ensemble classification models and a recurrent neural network model presented by the author in a previous paper (see Figure 4) with the physics Informed FDI models presented in this paper. This is to determine the performance of FDI models in detecting multi-component degradation scenarios when limited degradation data is available for model training. The Statistical Process Control, the ensemble and neural network models were trained with full degradation dataset in Table 2 simultaneously, tagged as models M_1, M_2 and M_3 respectively and stored in a Fault Detection and Isolation model repository. The function $f_2(x)$ is then used to determine the proportion of accurate predictions of test degradation scenario data by M_1, M_2 and M_3 .

A physics-informed Neural Network (PINN) enabled hybrid FDI algorithm is also developed in this report to detect multi component degradation scenarios. The hybrid model consists of a weighted average of a heuristic approximation model, a naïve recurrent neural network and a feedforward PINN model for each component in the water distribution system. The training of all models was done using randomly selected 0.05 % of the full degradation data from the original historical dataset used in Barimah et. al (2023) shown in Table 2. Figure 5 below shows the various cases in which the various randomly sampled degradation data can occur. Case A represents a scenario where part of the live process data from the system forms part of the distribution of the sampled random data. Case B is the non-ideal situation where the live process data is a subset of the sampled distribution while case

C is the ideal case where the degradation data available is truly limited. The rationale for the random approach is to reduce the quantity and diversity of degradation data available for model training and development hence the limited nature. This is done to determine the impact of limited data conditions on the performance of FDI algorithms in MCD scenarios. The levels of severity are categorized into two (2) groups with below 0.21 defined as healthy and between 0.21 and 1.0 defined a faulty in both MCD and SCD scenarios (see Figure 3). The performance of the FDI algorithms is measured using the interval ($0 \leq Performance \leq 1$) where 1 means the algorithm predicted correctly all the categorized severity states of the asset in operation while 0 means the algorithm failed to predict correctly any severity state of the asset.

3.3.1. Physics Informed Neural Network Model

As shown in Figure 2, five direct-acting proportional valves are used to emulate the dynamics of degradation patterns in the main components on the water distribution system. Equation (1) is used to determine the fluid flow through a valve where $f(V_0)$ is the function of valve opening with $0 \leq f(V_0) \leq 1$ as the interval for the valve opening and C_v is the valve coefficient (Knight, Russell, Sawalk & Yendell, 2013). Equations (2) & (3) are used to determine the level of severity $S(0,1)$ for blockages (Blocked Filter, degraded valve & Blocked Nozzle) and leakage (leaking pipe) respectively. For the pump, Eq. (4) is used to determine the severity level in a leaking pump degradation scenario for the gear pump on the testbed where N_v and N_m are the volumetric and mechanical efficiencies respectively. The maximum level of severity occurs when $S = 1$ with no fault condition being $S = 0$. Therefore, the interval of degradation for each component on the testbed is $0 \leq S \leq 1$ (see Figure 3).

$$flow = C_v f(V_0) \sqrt{\frac{\Delta P}{SG}} \tag{1}$$

$$S(0,1) = 1 - f(V_0) \tag{2}$$

$$S(0,1) = f(V_0) \tag{3}$$

$$S(0,1) = 1 - (N_m N_v) \tag{4}$$

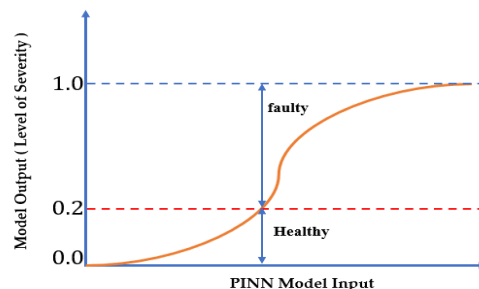


Figure 3. Change in component degradation severity level.

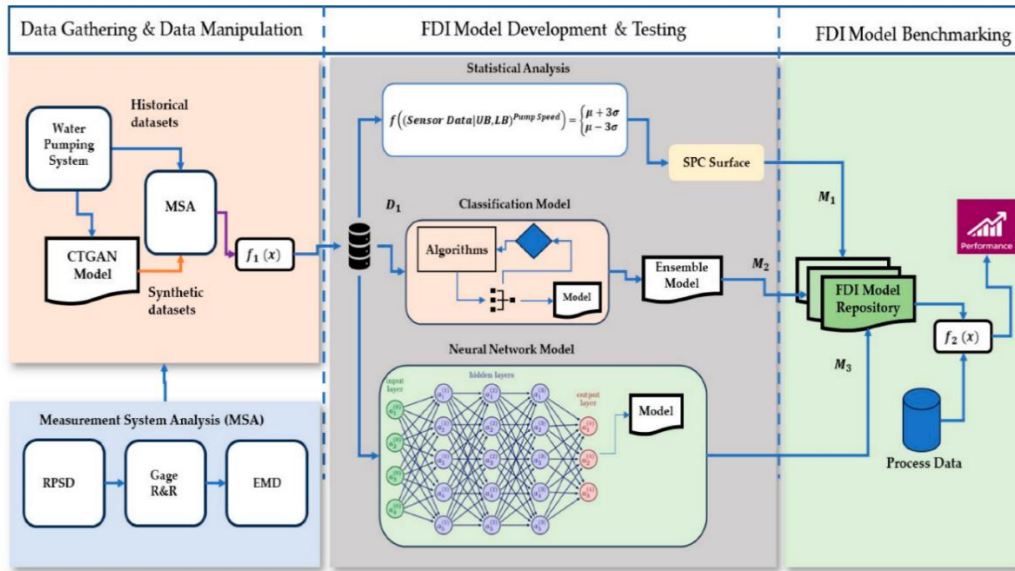


Figure 4. Proposed process for benchmarking the FDI algorithms (Barimah et. al 2023).

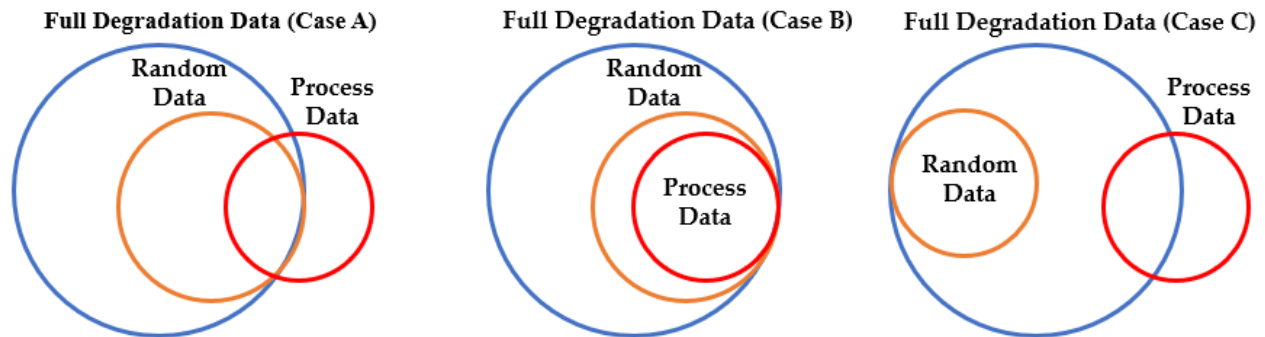


Figure 5. Random sampling of full degradation dataset for FDI model training.

Equations (2), (3) & (4) are used as physical constraints in constructing the loss function in the training process for the physics-informed neural network (PINN). Equation 2 is used for the filter, valve and nozzle all of which degrade via the gradual closing of DPV 1, DPV 3 and DPV 4 respectively. Since the gradual opening in DPV 5 represents a leakage in the main line, Eq. 3 is used to determine the extent of valve opening which represents the level of severity in the pipe. Equation (4) which represents the drop in gear pump volumetric efficiency when DPV 2 is opened is used in developing the loss function for the PINN model for the pump. The PINN model architecture used consists of a fully connected feedforward neural network with a Leaky version of the rectified linear unit (LeakyReLU) activation function to prevent any potential dying ReLU problem during the training process. The network has 1 input and output node, 3 hidden layers with 100 neurons in each layer. The Nadam

optimizer is used for its good coverage and faster training time (Bera & Shrivastava, 2020). A Mean Squared Error (MSE) Loss function of the PINN model $L(\theta)$ used is shown below where λ is a hyperparameter manually set to 1. Figure 6 below shows the PINN model architecture for each component on the testbed. The total loss for the PINN model which consists of the data and physics loss is shown in Equation (5). Table 3 also shows the various parameters used for the PINN model and the associated loss functions in Eqs. (6), (7) & (8) where $\beta = \frac{flow \times \sqrt{SG}}{C_v}$ and N_m are treated as trainable parameters in the training process.

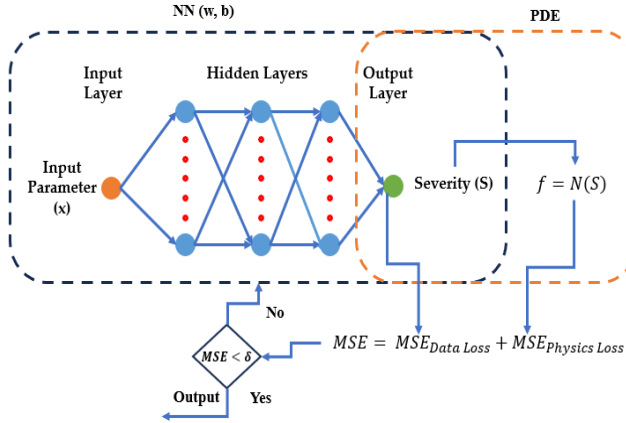


Figure 6. PINN Model Architecture for each component

$$Total\ Loss = (\lambda \times Data\ Loss) + Physics\ Loss \quad (5)$$

$$L_1(\theta) = \frac{\lambda}{N_b} \sum_{i=1}^{N_b} (S_{PINN}(x_i, \theta) - S_{obs}(x_i))^2 + \frac{1}{N_p} \sum_{j=1}^{N_p} \left(\left[V_0 - 1 + \left[\frac{\beta}{\sqrt{\Delta P}} \right] S_{PINN}(x_j, \theta) \right]^2 \right) \quad (6)$$

$$L_2(\theta) = \frac{\lambda}{N_b} \sum_{i=1}^{N_b} (S_{PINN}(x_i, \theta) - S_{obs}(x_i))^2 + \frac{1}{N_p} \sum_{j=1}^{N_p} \left([V_0 - 1 + N_m \cdot N_v] S_{PINN}(x_j, \theta) \right)^2 \quad (7)$$

$$L_3(\theta) = \frac{\lambda}{N_b} \sum_{i=1}^{N_b} (S_{PINN}(x_i, \theta) - S_{obs}(x_i))^2 + \frac{1}{N_p} \sum_{j=1}^{N_p} \left(\left[V_0 - \left[\frac{\beta}{\sqrt{\Delta P}} \right] \right] S_{PINN}(x_j, \theta) \right)^2 \quad (8)$$

Table 3. Parameters used for the construction of the PINN Model

Component	Learning Rate	λ	Input	Output	$L(\theta)$
Filter	1e-3	1	$\Delta P = P_2 - P_1 $	$S(0,1)$	$L_1(\theta)$
Valve	1e-3	1	$\Delta P = P_3 - P_4 $	$S(0,1)$	$L_1(\theta)$
Nozzle	1e-3	1	$\Delta P = P_5 - P_4 $	$S(0,1)$	$L_1(\theta)$
Pump	1e-3	1	N_p	$S(0,1)$	$L_2(\theta)$
Pipe	1e-3	1	$\Delta P = P_5 - P_4 $	$S(0,1)$	$L_3(\theta)$

3.3.2. Approximation Model

A heuristic model $S(0,1) = 1 - x_{O.C}$ is used to approximate the level of severity of both blockages and leakages (see Eqs. 10 & 11) in the system with a domain of [0,1]. The variable x is the feature of the component which is sensitive to a

change in degradation levels and it is defined as $x_{O.C}$ (see Eq. 9) with a domain of $x_{O.C} \in [0,1]$. The operating condition in this case is the speed of the pump.

$$x_{O.C} = \frac{Feature_{Operating\ Condition}}{Feature_{Healthy\ Condition}} \quad (9)$$

$$x_{O.C}(Blockage) = \frac{(Downstream\ Pressure / Upstream\ Pressure)_{Operating\ Condition}}{(Downstream\ Pressure / Upstream\ Pressure)_{Healthy\ Condition}} \quad (10)$$

$$x_{O.C}(Leakage) = \frac{|Downstream\ Pressure - Upstream\ Pressure|_{Operating\ Condition}}{|Downstream\ Pressure - Upstream\ Pressure|_{Healthy\ Condition}} \quad (11)$$

3.3.3. Recurrent Neural Network (RNN) Model

An FDI classifier based on a neural network architecture in a previous publication Barimah et. al (2023) which uses a recurrent neural network (RNN) architecture is used in this report. The RNN model comprises a single hidden layer with 150 neurons followed by a dense layer and a sigmoid activation function (see Figure 7 below). The model is compiled with binary cross-entropy loss and the Nadam optimizer. Early stopping is then employed to prevent overfitting during the training of the model.

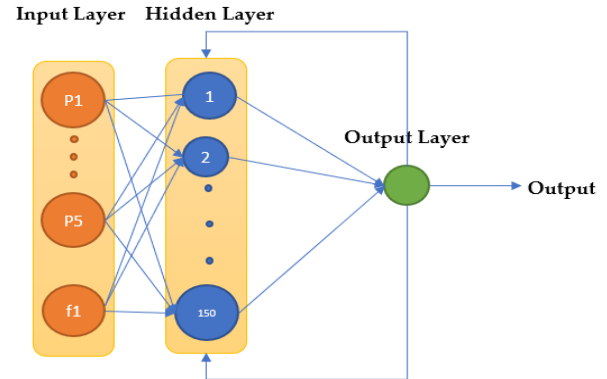


Figure 7. Recurrent Neural Network Architecture (Barimah et. al 2023)

3.3.4. PINN enabled Hybrid FDI Model

The physics-informed Neural Network (PINN) enabled hybrid FDI algorithm shown in Figure 8 is a weighted ensemble of the outputs of the RNN model, approximation model and PINN model. The weights of the model are skewed more towards the PINN model due to the limitations of purely data-driven model in the face of limited training data and its ability to generalize outside its training distribution. This PINN enabled hybrid model is then benchmarked against the other FDI algorithms, presented in Figure 4, for the system undergoing multi-component degradation scenarios. The model weights (W_D, W_P, W_A) for each component in the hybrid ensemble model are shown in Appendix B.

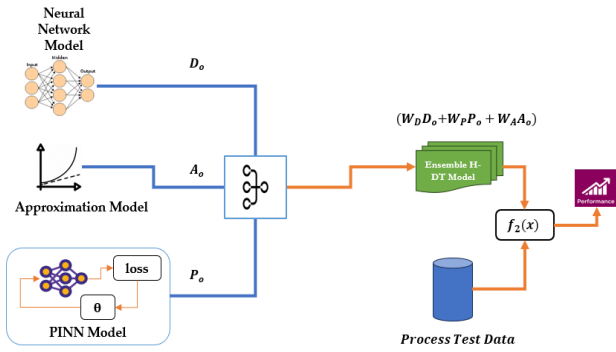


Figure 8. Ensemble Hybrid Framework for FDI models

3.3.5. Test Degradation Scenarios

Benchmarking is done using a series of test datasets recorded by Barimah et. al (2023) to assess the performance of FDI algorithms in the context of multi-component degradation. Table 3 below describes the nature of the test data with the components under consideration for the multi-component degradation scenarios, at different pump speeds, as well as their specific levels of severity.

Table 3. Test Degradation scenarios for FDI Model Testing

Dataset	Degradation (Component 1)	Degradation (Component 2)	Operational Speed Range (RPM)
T13	Pump (Medium-severity) at 45% DPV2 opening	Constant degradation of Nozzle: 30-70% DPV1 opening	700
T14	Pump (Medium-severity) at 45% DPV2 opening	Constant degradation of Nozzle: 30-70% DPV4 opening	950
T15	Filter (High severity) at 32% DPV1 opening	N/A	700 to 950
T16	Pump (Medium-severity) at 50% DPV2 opening	Nozzle (Medium-severity) at 40% DPV4 opening	700 to 950
T17	Constant degradation of Pump: 0-100% DPV2 opening	Constant degradation of Pipe: 0-100% DPV5 opening	800
T18	Intermittent faults for the pump between 45%-60% DPV2 opening	N/A	850

T19	Constant degradation of Pump: 0-100% DPV2 opening	Constant degradation of Valve: 30-70% DPV3 opening	850
T20	Pump (Medium-severity) at 55% DPV2 opening	Nozzle (High severity) at 30% DPV4 opening	700 to 950

4. RESULTS

4.1. Healthy Condition (HC) Scenario

The FDI algorithms showed very good performance in determining the healthy condition scenario in a situation where no fault had been injected into the system. Figure 9 shows the performance of all the FDI models in a healthy condition scenario with the pump speed at 700rpm and at 950 (see Appendix B). However, the performance of some of the models for components in a healthy state deteriorates once failure is introduced into the system. The performance of the FDI algorithms in faulty condition scenarios are presented in sections 4.2 to 4.4 showing the prediction of the conditions of various components on the testbed for the test scenarios.

4.2. Statistical Process Control (SPC)

The statistical process control (SPC) which relies on deviation from the mean of a process variable generally showed poor performance in the detection of the test MCD scenarios for components where faults were injected. For the test degradation scenario T13 which is has a leakage in the pump at DPV 2 of 45% opening and the gradual closure of DPV 4 which represents nozzle from 70% to 30%, the SPC model resulted in a 0.42 and 0.61 model performance for the pump and nozzle respectively (see Figure 9). In the case of T14 which has the same components under consideration but at a higher pump speed of 950rpm, the SPC showed an even poorer performance than in the case of T13 with 0.22 and 0.55 for the pump and nozzle respectively. However, for the components which had no failure injection, the SPC had a performance of 1.0 for the components not undergoing any form of degradation. This pattern of poor performance for components undergoing MCD scenarios and healthy components is seen in the rest of the test degradation scenarios T15, T16, T17, T18, T19 & T20 (see Appendix A).

4.3. Ensemble (Classifiers) and Recurrent Neural Network (RNN)

The ensemble classifier which uses the weighted outputs from logistic regression, support vector machine and decision tree classifier models also showed poor performance particularly for components not undergoing any form of degradation. This was revealed in T13 where it had a prediction performance of 0.42 for the pipe even though the pipe had no leak. This is also identified in T14 where the

model performance was 0.23 and 0.22 for the filter and pipe respectively. For components undergoing MCD scenarios the model showed some good performance for components (see Figure 10 & 11). The recurrent neural network (RNN) also showed a similar pattern of prediction to the SPC model albeit slightly better than the former. The performance of the RNN model of the nozzle deteriorates from 0.81 for T13 (700rpm) to 0.45 for T14 (950rpm). This drop in performance is also seen in the pump where the performance reduces from 0.42 to 0.22. For the test degradation scenarios T15, T16, T17, T18, T19 & T20 (see Appendix), the RNN model showed very good prediction for the components not undergoing degradation. Nonetheless, for the components undergoing the MCD scenarios, the RNN model showed mixed model prediction performance.

4.4. PINN enabled Hybrid FDI Model

The performance of the PINN enabled hybrid FDI model on the test degradation scenarios in Table 3 above showed improved performance compared to the other algorithms in the context of the MCD scenarios. Although the PINN model performs better than the other FDI models in the hybrid model, it sometimes underperforms as seen in T17 (see Appendix A4) where the weighted ensemble hybrid model compensates for the limitations in the PINN model in predicting the degradation of the leak in the pipe due to the impact of the other models in the hybrid model. For all the test degradation scenarios, the hybrid approach showed a much better performance as seen in Figures 10 & 11 as well as for test scenarios T15, T16, T17, T18, T19 & T20 (see Appendix A).



Figure 9. Performance of FDI algorithms for a Healthy Condition scenario at a pump speed of 700rpm.

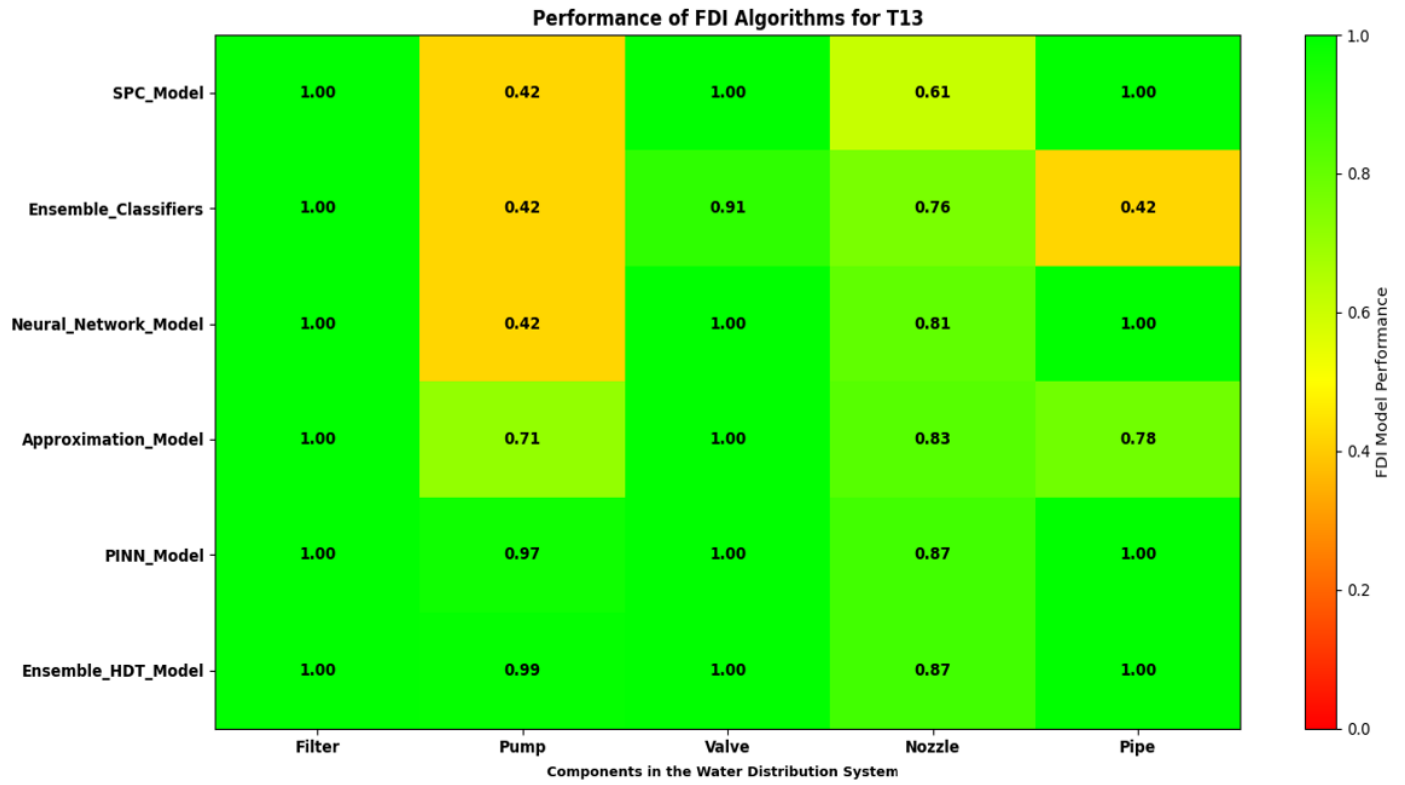


Figure 10. Performance of FDI algorithms on Test Degradation Scenario T13

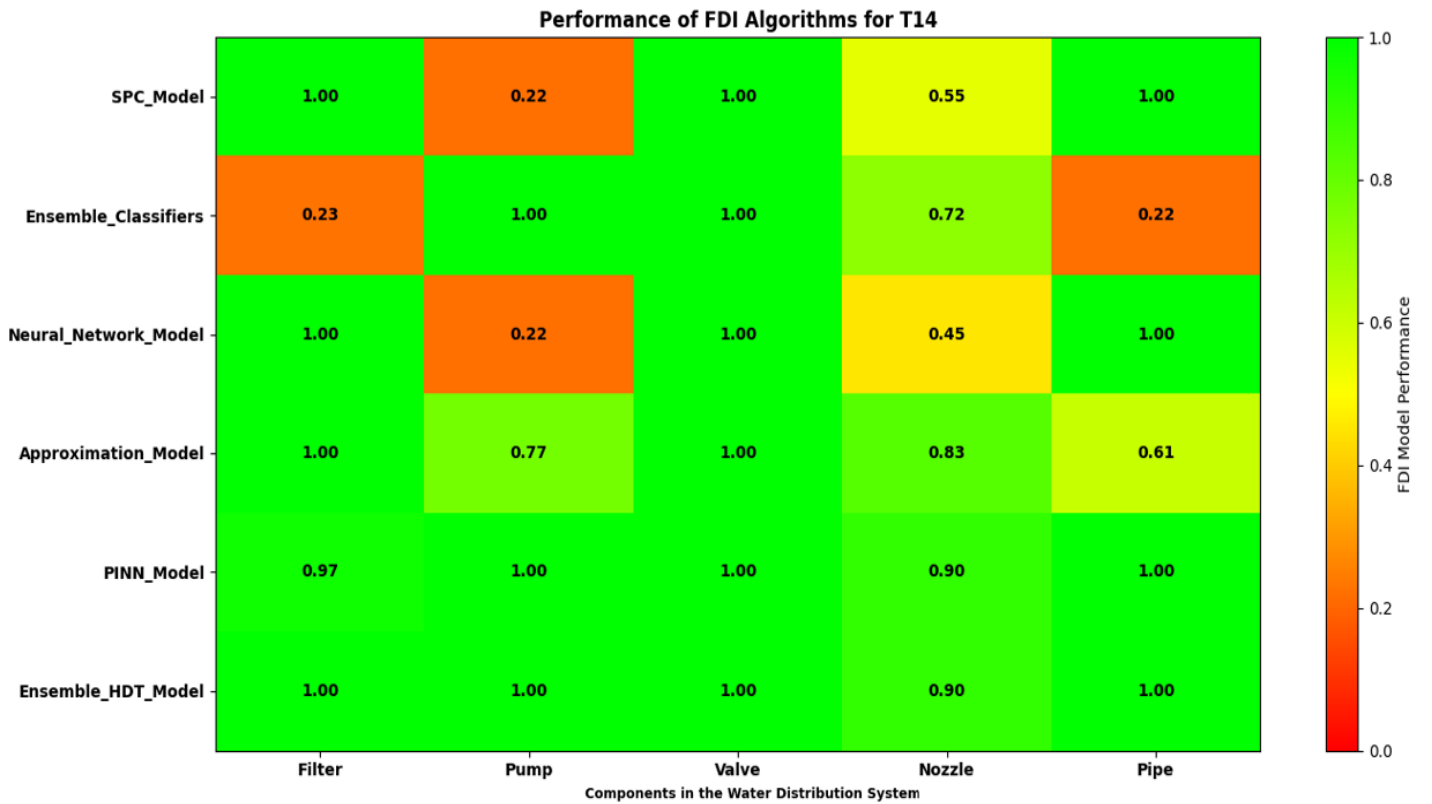


Figure 11. Performance of FDI algorithms on Test Degradation Scenario T14

5. DISCUSSION

For stakeholders in industry, training Fault Detection and Isolation models for PHM applications is key to optimizing asset health and logistics management. The challenge in model development as alluded to above is the availability of degradation data. The limited data available for training the FDI models presents a challenge in detecting MCD scenarios as seen in the results section above. The performance of the deep learning model for the test degradation scenarios showed the limitation in developing data-driven models on limited training data. This is seen in prediction of the state of the pump and nozzle in T13 & T17 as compared to the approximation and PINN models. However, it performs well when the training distribution of the available limited degradation data fall within the test degradation data scenario. This presents a challenge for stakeholders who have training data outside the distribution of the real time data from their assets. The ensemble hybrid approach proposed in Figure 8 compensates for this shortfall by integrating a heuristic approximation and a PINN approach with a neural network model to improve the overall model diagnostic performance. The main contributing parameters to the ensemble performance are the weights which were assigned using domain knowledge on the performance of the individual models with limited degradation data. This presents an interesting research opportunity for dynamically optimizing the weights in the ensemble hybrid model. The hybrid model also reduces the computational requirements for training the FDI models which ultimately reduces the cost for FDI model development for PHM applications.

6. CONCLUSIONS AND FUTURE WORK

In conclusion, this study highlights the capabilities of physics enabled fault detection and isolation algorithms for PHM diagnostics, emphasizing the challenges associated with limited training data and generalization issues. The proposed PINN-enabled hybrid model demonstrates promising FDI predictive capability for MCD diagnostics despite limited training data, indicating its potential for addressing the identification of multiple degraded conditions occurring simultaneously in a complex system. The contributions of the paper are:

C1. This study contributes to the application of physics informed FDI models for PHM applications in MCD scenarios, ultimately reducing model training data requirements for asset health management.

C2. The paper also presents an ensemble FDI approach with the capability of addressing the limitations of integrating both data-driven and physics based FDI models in multi-component degradation scenarios which can also be used in the analytics that drive digital twin applications. Future research would focus on dynamically optimizing ensemble hybrid model weights, leveraging prediction uncertainty to further enhance model performance.

NOMENCLATURE

<i>DT</i>	Digital Twins
<i>DPV</i>	Direct Proportional Valve
<i>FDI</i>	Fault Detection and Isolation
$L(\theta)$	Loss Function
<i>MCD</i>	Multi- Component Degradation
<i>NN</i>	Neural Network
<i>PHM</i>	Prognostic and Health Management
<i>PINN</i>	Physics Informed Neural Network
<i>RNN</i>	Recurrent Neural Network
<i>SCD</i>	Single Component Degradation
<i>SPC</i>	Statistical Process Control

REFERENCES

- Bararnia, H., & Esmaeilpour, H. (2022). On the application of physics informed neural networks (PINN) to solve boundary layer thermal-fluid problems. *International Communications in Heat and Mass Transfer*.
- Barimah, A., Niculita, I.-O., McGlinchey, D., & Cowell, A. (2023). Data-quality assessment for digital twins targeting multi-component degradation in industrial internet of things (IIoT)-enabled smart infrastructure systems. *Applied Science*, 13(24).
- Barimah, A., Niculita, O., McGlinchey, D., & Alkali., B. (2021). Optimal Service Points (OSP) for PHM enabled condition based maintenance for oil and gas applications. 6th European Conference of the Prognostics and Health Management Society.
- Bera, S. and Shrivastava, V.K., 2020. Analysis of various optimizers on deep convolutional neural network model in the application of hyperspectral remote sensing image classification. *International Journal of Remote Sensing*, 41(7), pp.2664-2683.
- Cai, S., Mao, Z., Wang, Z., Yin, M., & Karniadakis, G. (2021). Physics-informed neural networks (PINNs) for fluid mechanics. *A review. Acta Mechanica Sinica*, 1727-1738.
- Duriez, T., Brunton, S., & Noack, B. (2017). *Machine learning control-taming nonlinear dynamics and turbulence*. Cham: Springer.
- Higdon, D., Kennedy, M., Cavendish, J., Cafeo, J., & Ryne, R. (2004). Combining field data and computer simulations for calibration and prediction. *SIAM Journal on Scientific Computing*, 26(2), 448-466.

- Hu, Y., Miao, X., Si, Y., Pan, E., & Zio, E. (2022). Prognostics and health management: A review from the perspectives of design, development and decision. *Reliability Engineering & System Safety*, 217, 108063.
- Huang, B., & Wang, J. (2022). Applications of physics-informed neural networks in power systems-a review. *IEEE Transactions on Power Systems*, 38(1), 572-588.
- Knight, E., Russell, M., Sawalka, D. and Yendell, S., 2013. ValveModeling. Control Valve Wiki.
- Lu, Q., Xie, X., Parlikad, A., & Schooling, J. (2020). Digital twin-enabled anomaly detection for built asset monitoring in operation and maintenance. *Automation in Construction*, 118, 103277.
- Maass, W., Parsons, J., Purao, S., Storey, V., & Woo, C. (2018). Data-driven meets theory-driven research in the era of big data: Opportunities and challenges for information systems research. *Journal of the Association for Information Systems*, 19(2), 1.
- Rizi, S., & Abbas, M. (2023). From data to insight, enhancing structural health monitoring using physics-informed machine learning and advanced data collection methods. *Engineering Research Express*, 5(3), 32003.

BIOGRAPHIES

Atuahene Barimah is an Operations Assistant at Wellscope Energy Solutions and is currently a PhD researcher at Glasgow Caledonian University where he received his MSc. in Applied Instrumentation and Control at in 2020. He also received his BSc in Petroleum Engineering at the Kwame Nkrumah University of Science and Technology in 2017. His research interests include data-driven maintenance, system reliability, process control, project management, operations research, digital twin design, IIoT, and computational finance.

Octavian Nicolita is a Senior Lecturer in Instrumentation with Glasgow Caledonian University. He has a PhD in Industrial Engineering from the Technical University of Iasi,

Romania carried out under the EDSVS framework. His current research interests include industrial digitalization, predictive maintenance, PHM system design, integration of PHM and asset design for aerospace, maritime, and oil & gas (surface and subsea) applications. Octav has over ten years of experience in design and development of prognostics and health management applications, having worked on applied aerospace projects funded by The Boeing Company and BAE Systems as a Research Fellow and Technical Lead on his previous appointment with the IVHM Centre at Cranfield University, UK. He is a member of the Prognostics and Health Management Society, InstMC and the IET.

Don McGlinchey graduated from Strathclyde University with a BSc (Hons) Physics before working as a project engineer at Babcock Energy Ltd. He returned to academia and gained an MSc in Bulk Solids Handling Technology and his Doctorate on a study of the effect of vibration on powder beds. He is currently a Professor in the Department of Engineering at Glasgow Caledonian University where he is the academic leader in teaching, research, and consultancy in the area of multi-phase flow. He has edited two books, and authored over 100 papers, articles, and consultancy reports.

Andrew Cowell is the Chair of the Department of Engineering Industrial Advisory Group at Glasgow Caledonian University. In addition to his short-term contracts in research into coal handling for entrained flow gasifiers, and particulate solids handling education materials, Andrew has undertaken consultancy projects in the United Kingdom (UK), and delivered short courses in the USA, Sweden and the UK. He has also presented at international academic conferences in the UK, Australia, Norway and Spain. He is a Chartered Engineer, a Member of the IMechE and Fellow of the Institution of Engineers and Shipbuilders in Scotland.

Billy Milligan is the Director of Instrumentation and Control at Chart Industries. He has worked primarily on the design, testing and commissioning of screw compressor control systems within the oil and gas industry for the past 15 years. He is a member of the InstMC and the IET.

APPENDIX

Appendix A. FDI Model Performance

Figure A1. Healthy condition at 950 RPM



Figure A2. Test Scenario T15

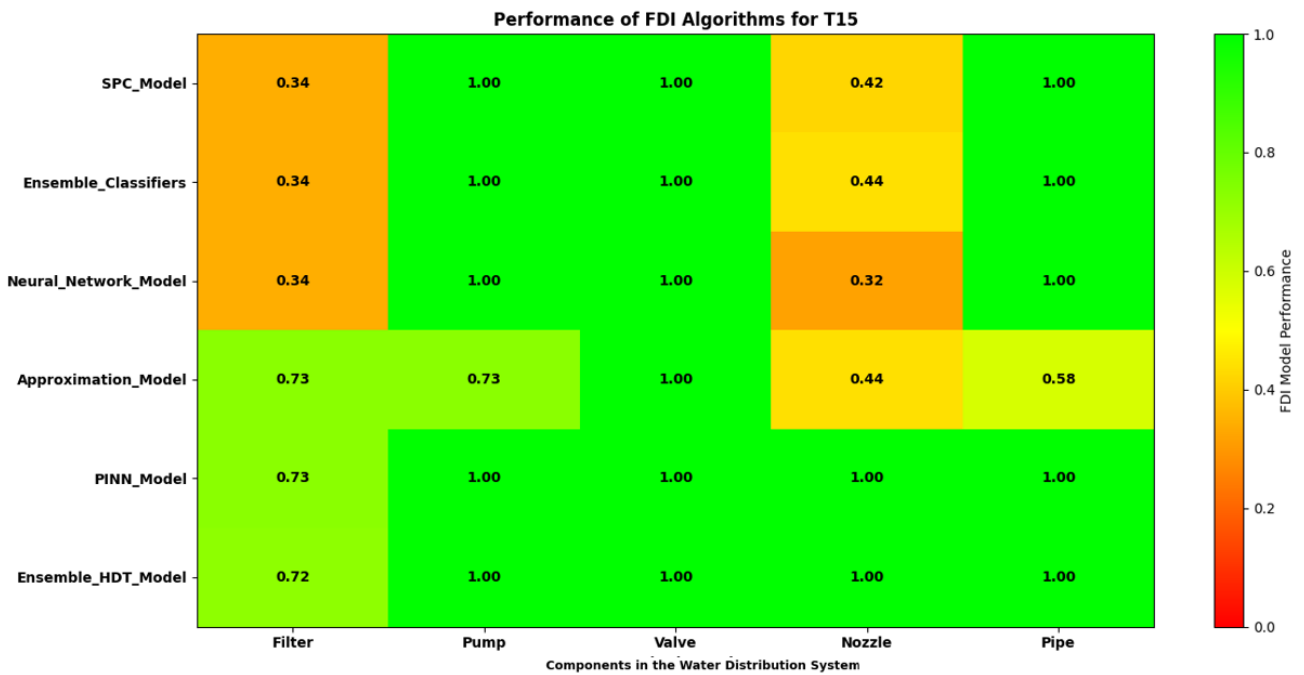


Figure A3. Test Scenario T16

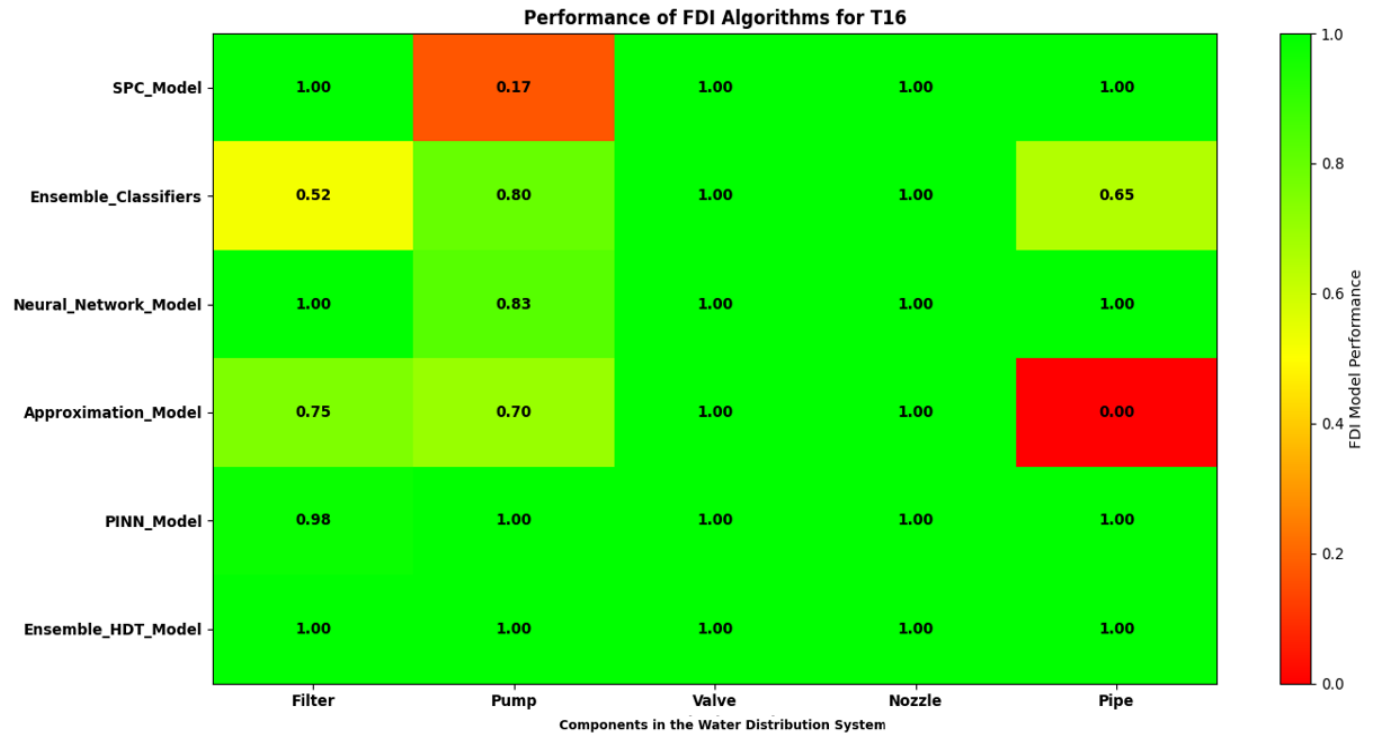


Figure A4. Test Scenario T17

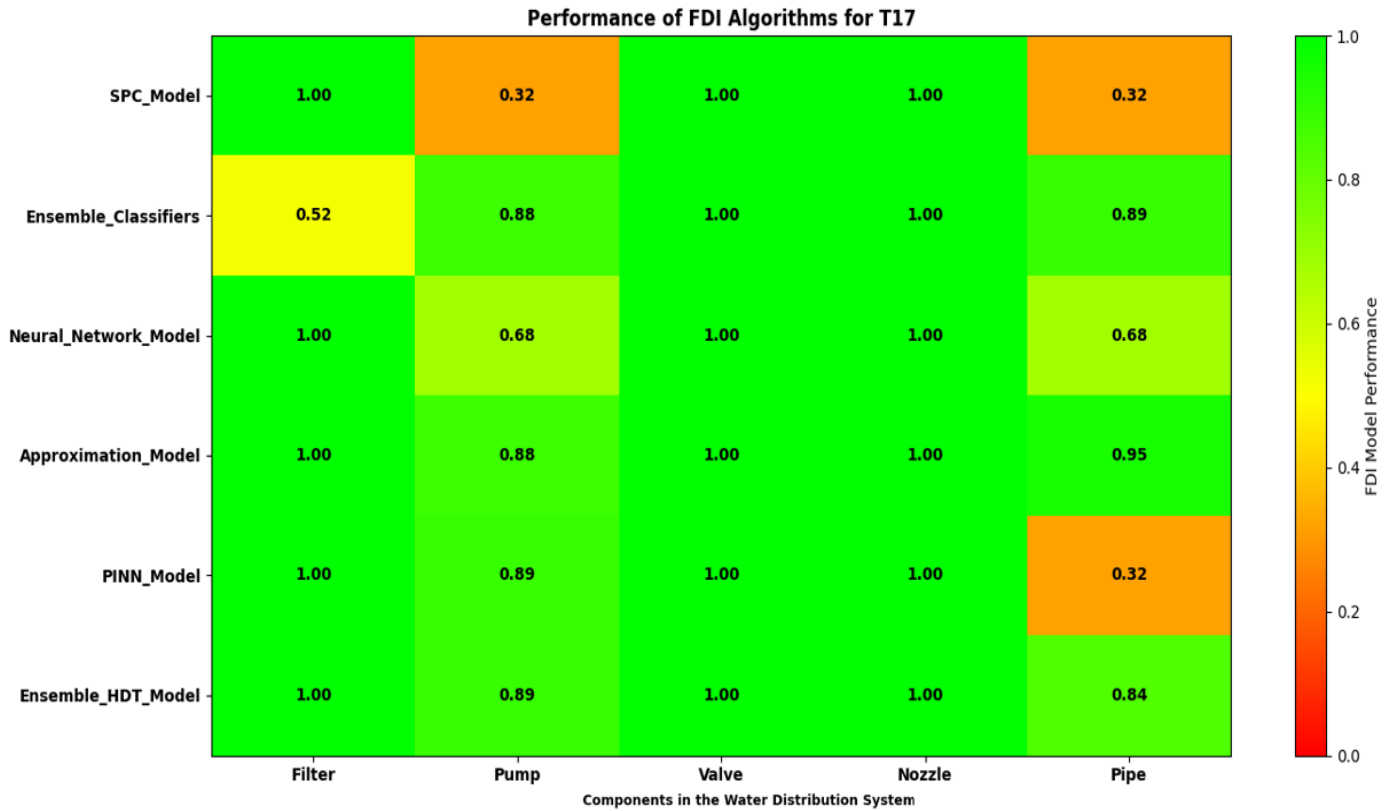


Figure A5. Test Scenario T18

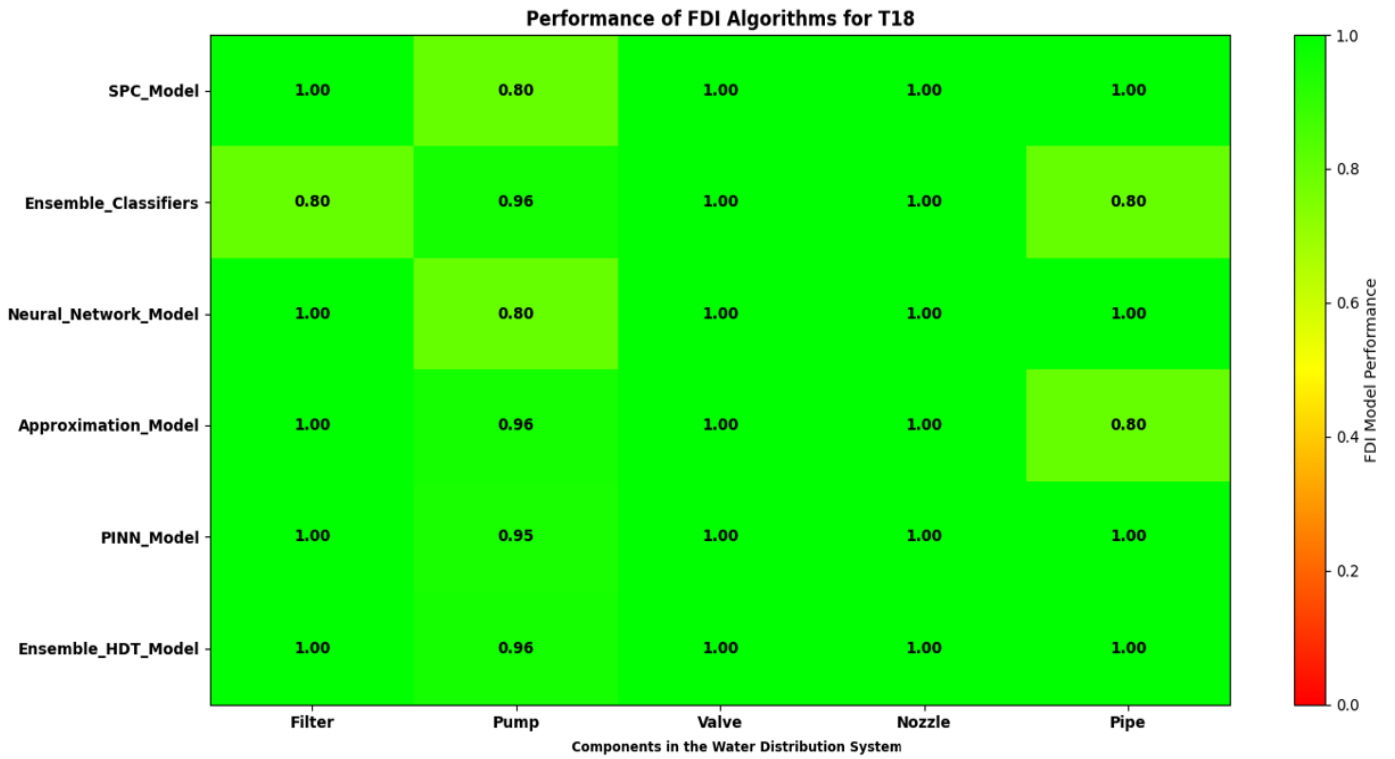


Figure A6. Test Scenario T19

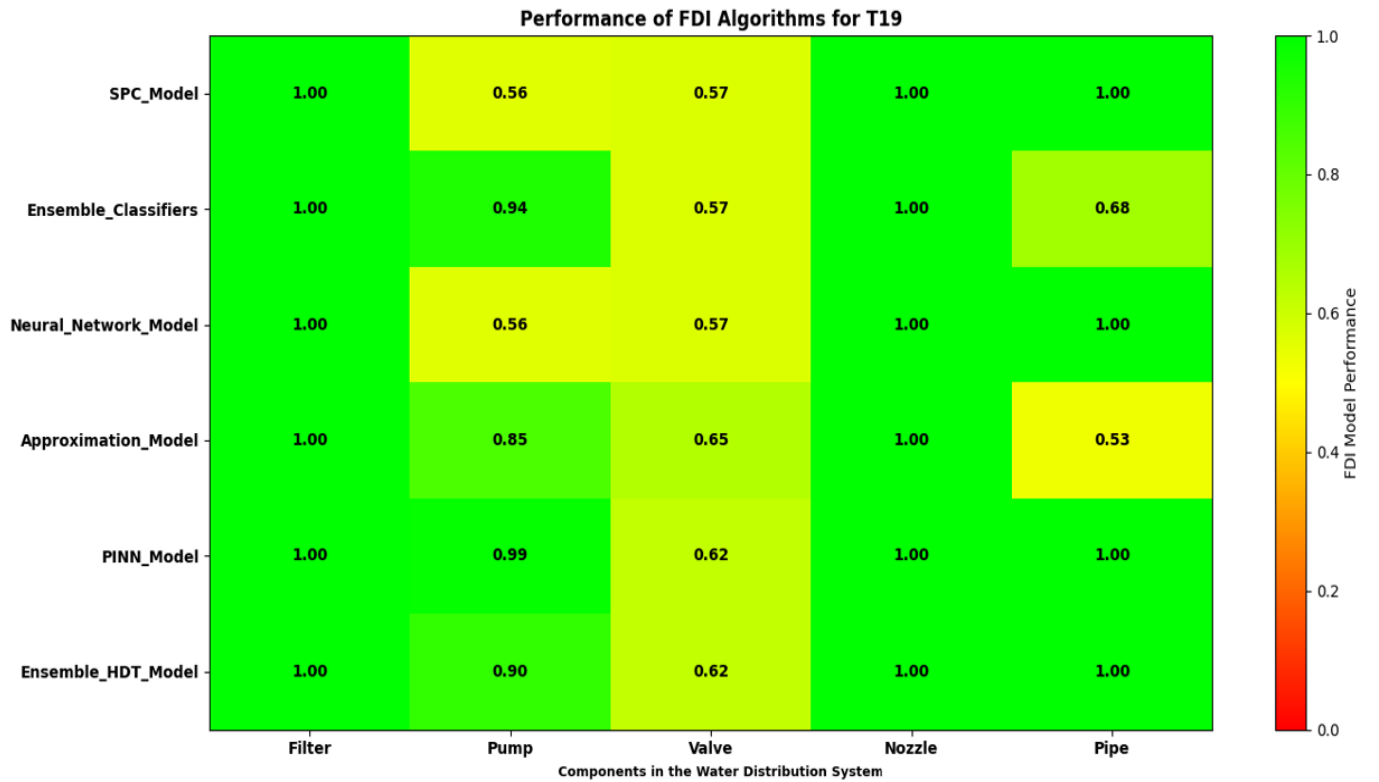
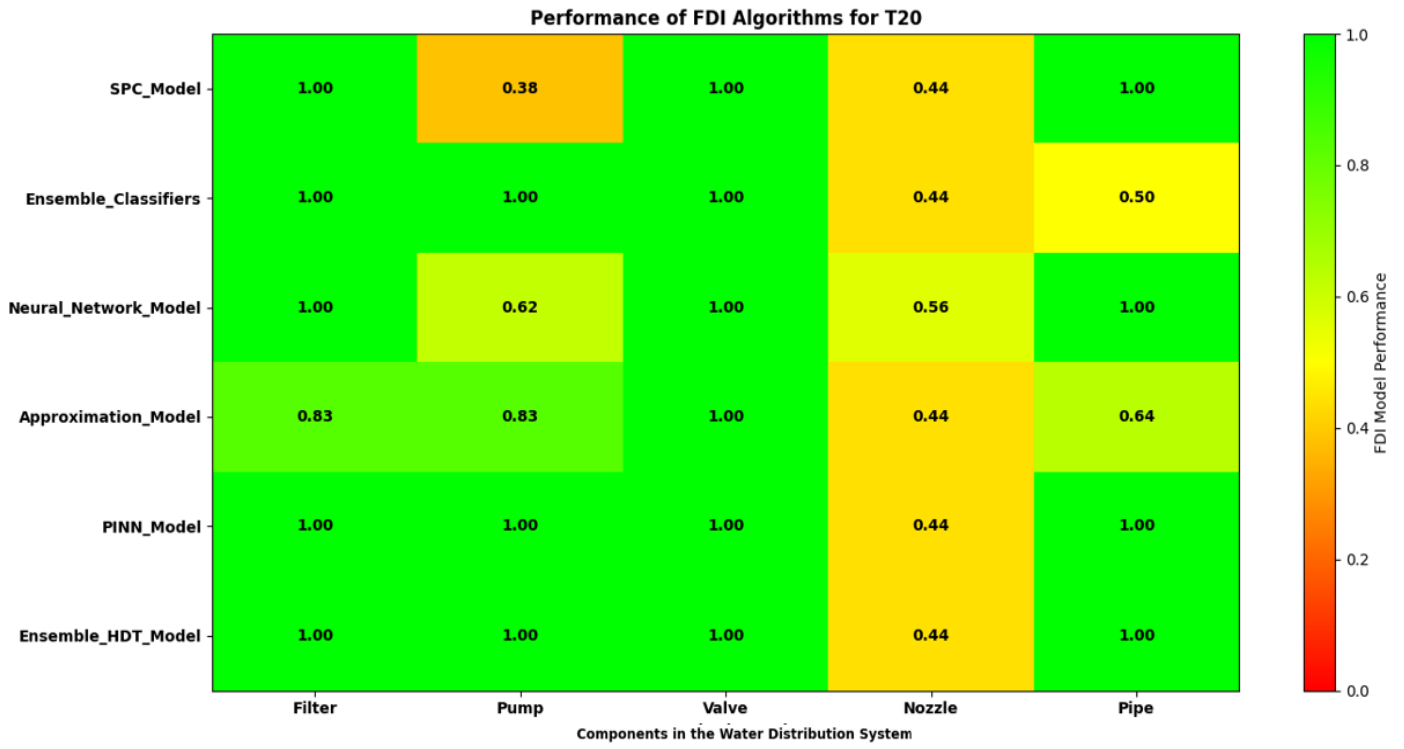


Figure A7. Test Scenario T20



Appendix B. Model Weights for FDI algorithms

